Journal of Vertebrate Paleontology

ISSN: 0272-4634 (Print) 1937-2809 (Online) Journal homepage: www.tandfonline.com/journals/ujvp20

Description of new *Kimmerosaurus langhami* (Cryptoclididae, Plesiosauria) material recovered from the Kimmeridge Clay Formation, Dorset, U.K.

Aubrey J. Roberts, Steve Etches, Nicholas Horton, John E. A. Marshall, Ian Harding, Kathryn Rankin & Neil J. Gostling

To cite this article: Aubrey J. Roberts, Steve Etches, Nicholas Horton, John E. A. Marshall, Ian Harding, Kathryn Rankin & Neil J. Gostling (05 Aug 2025): Description of new *Kimmerosaurus langhami* (Cryptoclididae, Plesiosauria) material recovered from the Kimmeridge Clay Formation, Dorset, U.K., Journal of Vertebrate Paleontology, DOI: 10.1080/02724634.2025.2505520

To link to this article: https://doi.org/10.1080/02724634.2025.2505520

Journal of Vertebrate Paleontology e2505520 (15 pages)

DOI: 10.1080/02724634.2025.2505520

ARTICLE

DESCRIPTION OF NEW *KIMMEROSAURUS LANGHAMI* (CRYPTOCLIDIDAE, PLESIOSAURIA) MATERIAL RECOVERED FROM THE KIMMERIDGE CLAY FORMATION, DORSET, U.K.

AUBREY J. ROBERTS, *[1,2] STEVE ETCHES,[3] NICHOLAS HORTON,[4] JOHN E. A. MARSHALL,[4] IAN HARDING,[4] KATHRYN RANKIN,[5] and NEIL J. GOSTLING[6]

[1]Natural History Museum, University of Oslo, Sars' Gate 1, 0562 Oslo, Norway a.j.roberts@nhm.uio.no;
[2]Department of Earth Sciences, The Natural History Museum, Cromwell Road, London SW7 5BD, U.K.;
[3]The Etches Collection Museum of Jurassic Marine Life, Kimmeridge, Dorset BH20 5PE, U.K., steve.etches@theetchescollection.org;
[4]School of Ocean and Earth Science, Faculty of Environmental and Earth Science, University of Southampton, Southampton SO14 3ZH, U.K., jeam@soton.ac.uk;
[5]μ-VIS X-ray Imaging Centre, Faculty of Engineering and Physical Sciences, University of Southampton, Southampton SO17 1BJ, U.K., k.rankin@soton.ac.uk;
[6]School of Biological Sciences, Faculty of Life and Environmental Sciences, University of Southampton, Southampton SO17 1BJ, U.K., n.j.gostling@soton.ac.uk.

ABSTRACT—A new specimen of the cryptoclidid plesiosauroid *Kimmerosaurus langhami* (EC K2134) is described from the Upper Jurassic Kimmeridge Clay Formation, Kimmeridge Bay, Dorset, U.K. We provide new insights into the cranial morphology of this taxon, and significantly, we report the discovery of the first cryptoclidid hyoid, a useful comparative element for future studies. Comprehensive investigations into the anatomy and paleobiology of *Kimmerosaurus langhami* have been hampered by the scarcity of relevant fossil material. The previous cranial reconstruction of *Kimmerosaurus* was based on incomplete skull material consisting of part of the skull roof, brain case, dentary, teeth, and vertebrae. Using computed tomography (CT) scanning, we provide high-resolution 3D images of the new material, adding the rostrum, palate, and revised tooth count to the reconstruction. In addition, this new material provides significant insights into the cranial and anterior cervical morphology of *K. langhami*. Phylogenetic results support the referral of the specimen, placing EC K2134 in a polytomy with the North American taxon *Tatenectes laramiensis* and known material of *K. langhami*. This study highlights the use of computed tomography for description of Kimmeridge Clay fossil material.

SUPPLEMENTARY FILES—Supplementary files are available for this article for free at www.tandfonline.com/UJVP.

Citation for this article: Roberts, A. J., Etches, S., Horton, N., Marshall, J. E. A., Harding, I., Rankin, K., & Gostling, N. J. (2025) Description of new *Kimmerosaurus langhami* (Cryptoclididae, Plesiosauria) material recovered from the Kimmeridge Clay Formation, Dorset, U.K. *Journal of Vertebrate Paleontology*. https://doi.org/10.1080/02724634.2025.2505520

Submitted: December 4, 2023
Revisions received April 11, 2025
Accepted: April 25, 2025

INTRODUCTION

The order Plesiosauria were an extinct group within the subclass Sauropterygia, which was composed of large and mainly predatory marine reptiles (Benson & Druckenmiller, 2014; Massare, 1987). Their first records appear in the Late Triassic (Wintrich et al., 2017), and they rapidly achieved a global distribution until their final extinction at the end of the Cretaceous (Mulder et al., 2000; Vincent et al., 2011). The Jurassic saw the rise of two main body forms, classically dividing them into two groups (Welles, 1943). In recent years, these forms have been shown to have evolved multiple times independently (Bakker, 1993; Benson et al., 2012; Benson & Druckenmiller, 2014; Ketchum & Benson, 2010; O'Keefe, 2001, 2002) and so the term "morph," is utilized when referring to body shape. "Plesiosauromorphs" comprises taxa with long necks and small skulls, while "pliosauromorphs" include taxa with large, elongated skulls and shortened necks (O'Keefe, 2002). In the Middle–Late Jurassic one of the most prevalent plesiosaurian family were the crytptoclidids (Brown, 1981).

Cryptoclididae represents a family of Middle Jurassic to Early Cretaceous plesiosaurs. They achieved a cosmopolitan distribution by the Late Jurassic, with specimens recovered on a global scale, e.g., the U.S.A. (O'Keefe & Street, 2009; O'Keefe & Wahl, 2003), Chile (Otero et al., 2020), European Russia (Arkhangelsky et al., 2020), Cuba (Gasparini et al., 2002), and Svalbard (Knutsen et al., 2012a, 2012b, 2012c; Roberts et al., 2020). However, the Kimmeridge Clay Formation (KCF) and Oxford Clay Formation (OCF) in the U.K. is noteworthy for

*Corresponding author.

Color versions of one or more of the figures in the article can be found online at www.tandfonline.com/ujvp.

Published online 05 Aug 2025

yielding the most and some of the earliest discoveries of the family (Brown, 1981; Owen, 1869). Although four morphotypes of cryptoclidid plesiosaurs have been recognized from the KCF based on cervical material (Benson & Bowdler, 2014), one of the more recent additions to this family from the KCF is *Kimmerosaurus langhami*, initially described from an incomplete cranium (Brown, 1981).

Since its initial description, only two additional specimens of *Kimmerosaurus langhami* have been described, the first consisting of the mandible, braincase, and five cervical vertebrae (NHMUK R. 10042; Brown et al., 1986), the second of a partial skull and mandible (NHMUK R.1798; Brown et al., 1986). The new *K. langhami* material presented in this paper from the Etches Collection (Dorset, U.K.), allows us to add more information to this poorly known taxon. The specimen (EC K2134) includes a near-complete disarticulated skull and several cervical vertebrae. Using micro-computed tomography (μ-CT), we have been able to reconstruct the morphology of this specimen and used it to modify Brown's (1981) original skull reconstruction. Our contributions to the new skull reconstruction include the premaxilla, maxilla, part of the skull roof and palate, as well as cranial elements expanding the species diagnosis by Brown (1981) and Brown et al. (1986). In addition, we present evidence of hyoids for the first time in cryptoclidid plesiosaurs. Although there are some differences between EC K2134 and the type specimen of *K. langhami* (see Discussion), they are not distinct enough to warrant a new species.

Geological Setting

The Kimmeridge Clay Formation (KCF) is a thick sequence of alternating, thinly laminated calcareous and bituminous mudstones interbedded with thin dolostone and limestone horizons from the Late Jurassic and ranging in age from 145–155 Ma (Hesselbo et al., 2020). Named after the type area of Kimmeridge Bay in South Dorset, the outcrop stretches north-east to Yorkshire with a subcrop extending across much of the southern English coast. The formation has become an abundant source of Jurassic vertebrates including both terrestrial and marine specimens, with several well-preserved examples of Jurassic plesiosaurs. Ammonites are abundant, with the former providing detailed biostratigraphy for the Kimmeridgian Stage.

The cyclicity of the alternating laminated calcareous and very organic rich bituminous mudstones at Kimmeridge is interpreted to record orbital obliquity and precession from their influence on bottom water oxygenation and terrestrial runoff (Morgans-Bell et al., 2001; Weedon et al., 2004). The mudstones were deposited on a shallow continental marine shelf distant from the shore and with a water column that was generally anoxic and euxinic with framboidal pyrite formation (Pearson et al., 2004). A significant component of these mudstones is carbonate produced by coccoliths and transported to the seafloor in fecal pellets. Superimposed on these dominant anoxic conditions were short episodes when oxic conditions prevailed and there was limited colonization of the sea floor by benthic organisms, particularly bivalves. The microscopic terrestrial organic matter within the mudstones is well mixed and points to storms as a constant process that provided limited seasonal mixing in the water column. At times the dominantly mudstone depositing environment switched to entirely coccolith production probably from suppression of the anoxic water column and this resulted in deposition of distinct coccolith limestones. Specimen EC K2134 was collected *ex situ*, washed off an offshore shale reef onto the shore, likely originating out of *Pectinatites pectinatus* zone of the Upper Kimmeridge Clay (Pearson et al., 2004). Detailed cyclostratigraphic analysis of the Kimmeridge Clay (reviewed in Hesselbo et al., 2020) provides an age of ~147 Ma for this ammonite zone.

MATERIALS AND METHODS

Specimen EC K2134 was found almost entirely embedded in the rock matrix with parts of only two vertebrae and elements of the braincase largely free from the rock and the outline of the lower jaw visible. The subsequent excavation of the dorsal side of the block revealed that most of the skull was preserved. Following the μ-CT scan the ventral side of the block was air abraded to reveal the block in its current state. In this specimen most of the elements are disarticulated, with only the posterior regions of right mandible and fused sections of skull in articulation. EC K2134 was prepared at the Etches Collection.

Specimen EC K2134 is held at the Etches Collection (Jurassic Museum of Marine Life) which is a publicly accessible institution. The specimen is owned by the Kimmeridge Trust as a charitable trust (United Kingdom Charity number 1106638). The specimens are not in private ownership.

Computed Tomography Methodology—Specimen EC K2134 was micro-Computed Tomography (μ-CT) scanned at the μ-VIS X-ray Imaging Centre (University of Southampton, U.K.) using a custom built, dual source 225/450 kV walk-in room (Nikon Metrology, U.K.) with a micro-focus 450 kV source (fitted with a tungsten reflection target) and a Perkin Elmer XRD 1621 CN03 HS detector. The specimen block was fixed with screws to a plywood board, approximately 300 × 10 × 600 mm. This allowed the fragile specimen to be securely mounted in the vertical orientation on the rotate stage, such that it rotated about its longest axis, with the fossil centered in the field of view (FOV). Micro-CT scans were conducted at a peak voltage of 320 kVp and power of 121 W, with a source to object distance of 807 mm and a source to detector distance of 1198 mm, giving an FOV of 269.5 mm. The imaging conditions used 18 dB analogue gain with binning 2 of the 2000 × 2000 pixel detector to improve signal to noise ratio. The scan acquired 1571 projection images through 360° rotation, averaging 32 frames per projection with an exposure time of 177 ms (per frame). Two scans were acquired to cover the height of the region of interest within the block (429.6 mm).

The projection data were reconstructed into 1000 × 300 × 1000 voxel (cubic pixel) 32-bit float volumes with a voxel resolution of 0.269 mm, using filtered back-projection algorithms implemented within CTPro3D and CTAgent software v2.2 (Nikon Metrology, U.K.). These were then concatenated using ImageJ/Fiji (Rasband, W.S., ImageJ, U.S.A., National Institutes of Health, Bethesda, Maryland, U.S.A., https://imagej.nih.gov/ij/, 1997-2019) and down-sampled to 8 bit to reduce data processing time. Segmentation work was completed in Avizo (2020.2) at the University of Southampton (μ-VIS) and version (2020.2) at the University of Oslo Natural History Museum. Selected measurements of individual elements were taken from the μ-CT data in Avizo (2020.2), these are available in the Supplementary File 1 (Table S1).

Phylogenetic Data and Methods—Specimen EC K2134 was scored as a separate OTU (operational taxonomic unit) into the matrix by Benson and Druckenmiller (2014) using the updated and modified matrix published in Roberts et al. (2020). The total matrix contains 77 OTUs, with 273 characters. Nine scorings for *Kimmerosaurus langhami* were modified based on observations on the type and referred material held at the NHMUK (see Supplementary File 1 for list and justification). The matrix was edited in Mesquite (Maddison & Maddison, 2023) and analysed in TNT (V.1.6; Goloboff & Morales, 2023), following the methodology in Roberts et al. (2020). The NEXUS file is deposited at Morphobank (Project 5825). All characters were treated as unordered and equally weighted. The taxon *Yunguisaurus liae*, was utilized as the outgroup in the analysis. This involved using a New Technology Ratchet search with 1000 replications (10 random seed, 10 random

addition sequences, keep all trees). A heuristic search (TBR-Tree bisection reconnection) was subsequently completed on the trees found in the ratchet analysis. The consistency index (CI) and retention index (RI) were calculated using a script (stats.run), which had been edited by Roberts et al. (2020) to work on more trees. Bremer support was completed using the bremer.run script and the resulting values are displayed above branches. Bootstrap analysis run with 1000 replications using the traditional algorithm showed all nodes with a support of <50 for Cryptoclididae and are as such not displayed. A complete tree is available in Supplementary File 1 (Fig. S4) with support values for all nodes.

Institutional Abbreviations—CAMSM, Sedgwick Museum of Earth Science, Cambridge University, Cambridge, U.K.; **EC**, The Etches Collection, Kimmeridge, Dorset, U.K.; **GLAHM**, The Hunterian Museum, University of Glasgow, Glasgow, U.K.; **LEICS**, Leicester New Walk Museum, Leicester, U.K.; **MANCH**, The Manchester Museum, Manchester, U.K.; **NHMUK**, Natural History Museum, London, U.K.; **NOTNH**, Wollaton Hall, Nottingham, U.K.; **OUM**, Oxford University Museum of Natural History, Oxford, U.K.; **PETRM**, Peterborough Museum, Peterborough, U.K.; **PMO**, Paleontological Museum Oslo, University of Oslo, Oslo, Norway; **UW**, University of Wyoming, Wyoming, U.S.A.

SYSTEMATIC PALEONTOLOGY

SAUROPTERYGIA Owen, 1860
PLESIOSAURIA de Blainville, 1835
CRYPTOCLIDIDAE Williston, 1925
KIMMEROSAURUS Brown, 1981

Type [and Only] Species—*Kimmerosaurus langhami* Brown, 1981.

Holotype—NHMUK R.8431.

Referred Specimens—NHMUK R.1798; NHMUK R.10042; EC K2134.

Emended Diagnosis for *Kimmerosaurus* from Brown et al., 1986—A cryptoclidid with the following autapomorphic features: tooth ornament absent; premaxilla bears eight alveoli; maxilla bears 32 alveoli; dentary bears 36 alveoli; parietals do not form a sagittal crest forming instead a mediolaterally wide table. *Kimmerosaurus langhami* can be differentiated from other cryptoclidids by the following combination of characters: teeth greatly recurved, sharply pointed and labiolingually compressed; the premaxilla bears mild pitting on the dorsal surface; maxillary alveoli vary slightly in size and lateral extension; maxilla lateral surface smooth; basioccipital tubera have limited articulation to the basisphenoid; a short anteromedial process of the pterygoid present reaching a facet on the basisphenoid; clear laterally projecting basal articulation of the parasphenoid; occipital condyle not ringed by a groove and extends onto the pedicels of the exoccipitals*; quadrate overlaps quadrate ramus of the pterygoid anterolaterally; the quadrate lateral condyle is subtly larger than the medial condyle; anteroposteriorly elongated hypapophyseal eminence positioned posteroventrally; vertebrae have amphicoelous centra, the shape of a cross section of the articular face being a double sigmoid curve; length of anterior cervical centra less than height.

*feature absent in EC K2134 and referred specimen NHMUK R.17988.

Diagnostic Remarks on EC K2134—The new specimen of *Kimmerosaurus langhami* (EC K2134) is referred to the genus on the basis of the emended diagnosis by Brown et al. (1986): the basioccipital tubera have limited articulation to the basisphenoid; quadrate overlaps quadrate ramus of the pterygoid anterolaterally; anteromedial process of the pterygoid present (as suggested for genus in Benson & Druckenmiller, 2014; Roberts et al., 2020); vertebrae have amphicoelous centra, the shape of a cross section of the articular face being a double sigmoid curve; length of anterior cervical centra less than height.

In addition, EC K2134 demonstrates the estimated number of alveoli in the premaxilla (8) and maxilla (>28) as suggested by Brown et al. (1986).

Occurrence—Upper part of *Eastlecottensis* Subzone, *Pectinatus* Zone. Upper Kimmeridge Clay.

DESCRIPTION AND COMPARISON

Skull

The skull of EC K2134 is disarticulated and includes a premaxilla, maxilla, fragment of other maxilla, pterygoids, squamosals quadrates, fragments of the skull roof and/or palate, braincase, mandible, and a single hyoid (Figs. 1–5; Supplementary File 1, Fig. S1). Selected measurements can be found in the Supplementary File 1 (Table S1).

Premaxilla—Two large fragments of the left premaxilla are for the first time described for *Kimmerosaurus langhami*. Although significantly compressed and damaged due to contact with the dentary, some important features can be noted. Based on the preservation of the maxilla, the premaxilla may contribute to the external naris as described for in *Muraneosaurus leedsii* and *Tricleidus seeleyi* (Andrews, 1910; Brown, 1981). The preorbital to total skull length ratio is estimated to be 0.40 similar to 0.43 in *Ophthalmothule cryostea* (Roberts et al., 2020). This was estimated for EC K2134 by the length of the premaxilla, preorbital maxilla and lower jaw. There are eight alveoli (Figs. 3, 5A; Supplementary File 1, Fig. S1), agreeing with the minimum of eight estimated by Brown (1981), differing from the five in *M. leedsii* (Andrews, 1910), six in *Cryptoclidus eurymerus* (Brown, 1981) and *O. cryostea* (Roberts et al., 2020). This is the highest number of premaxillary alveoli described for cryptoclidid plesiosaurs and represents a clear apomorphy of this taxon (Brown, 1981). Despite the poor preservation, the alveoli appear to be uniform in shape. However, the 3rd and 4th alveoli appear slightly larger than the anterior and posterior alveoli. The premaxilla/maxilla suture can be identified just posterior of the 8th alveolus as being angled posterodorsally. Similar, but not as distinct as in *O. cryostea* (Roberts et al., 2020), a dorsoventrally thickened area suggests the presence of a low anteroposterior ridge between the premaxillae. This feature is described as absent in *C. eurymerus* (Brown & Cruickshank, 1994), although low ridge does seem to be present anteriorly in one specimen of *C. eurymerus* (PETMG 283.411). As in *M. leedsii* (NHMUK R2421, Andrews, 1910), the dorsal surface of the premaxilla shows small, shallow pits (Fig. 2), these are significantly reduced in comparison to that seen in *O. cryostea* (Roberts et al., 2020) and *Tricleidus seeleyi* (Andrews, 1910). Dentition is missing from this element.

Maxilla—Specimen EC K2134 preserves a near-complete right maxilla, which is here figured in ventral (Figs. 1, 3) and dorsal (Fig. 2; Supplementary File 1, Fig. S1) views. The left maxilla is only preserved in fragments, as such the right maxilla is used for the description. The degree of compression of the right maxilla is unclear, but some features, such as the dorsal process are clearly distorted. The maxilla bears a total of 32 alveoli, greater than the minimum estimate of 26 teeth based on the mandible by Brown (1981). This is significantly more than described in other cryptoclidids (16 in *Muraenosaurus leedsii*, Brown, 1981; 15 in *Tricleidus seeleyi*, Brown, 1981; 18 in *Cryptoclidus eurymerus*, Brown, 1981; maximum of 16 in *Ophthalmothule cryostea*, Roberts et al., 2020). Contrasting to *T. seeleyi* (Brown, 1981), the alveoli of EC K2134 vary only slightly in morphology and size as in *O. cryostea* (Roberts et al., 2020). Larger alveoli are present anteriorly, with smaller alveoli posteriorly.

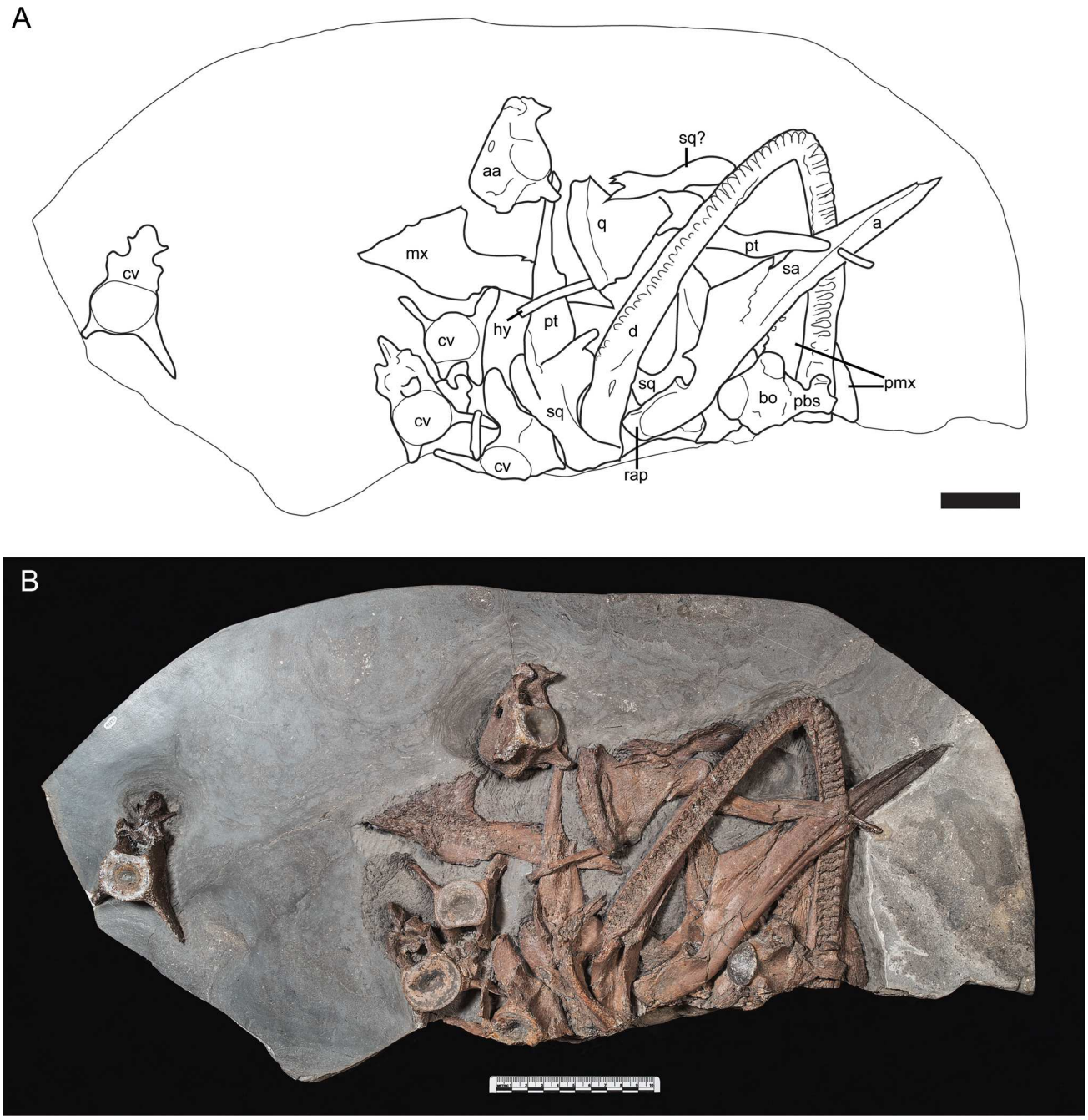

FIGURE 1. The disarticulated skull and cervicals of EC K2134. **A**, interpretation of bone elements; **B**, photograph of specimen. **Abbreviations**: **a**, angular; **aa**, atlas axis; **bo**, basioccipital; **cv**, cervical vertebra; **d**, dentary; **hy**, hyoid; **mx**, maxilla; **pbs**, parabasisphenoid; **pmx**, premaxilla; **pt**, pterygoid; **q**, quadrate; **rap**, retroarticular process; **sa**, surangular; **sq**, squamosal. Scale bar equals 5 cm.

Particularly the anterior and posterior alveoli show a clear lateral-facing orientation. The lateral-facing alveoli resemble somewhat those of the elasmosaurids *Aristonectes parvidens* (Gasparini et al., 2003) and *Morturneria seymourensis* (O'Keefe et al., 2017), which display interlocking combs of needle-like teeth that occluded outside the mouth. In lateral view, based on the large dorsal process of the maxilla, it is likely that the maxilla contributed to the ventral and anterior margin of the orbit, as well as the posterior and posteroventral margins of the external naris. This morphology is clear on the completely prepared side of the specimen (Fig. 1). Due to the preservation, it is uncertain if the maxilla contributes to the internal naris. The lateral surface of the maxilla is not pitted, unlike *O. cryostea* (Roberts et al., 2020). On the medial surface there is a dorsoventrally oriented circular structure, angled posteriorly. It is uncertain how much of this reflects real taphonomy or deformation but it could potentially represent the position for articulation to the vomer and/or palatine as described in

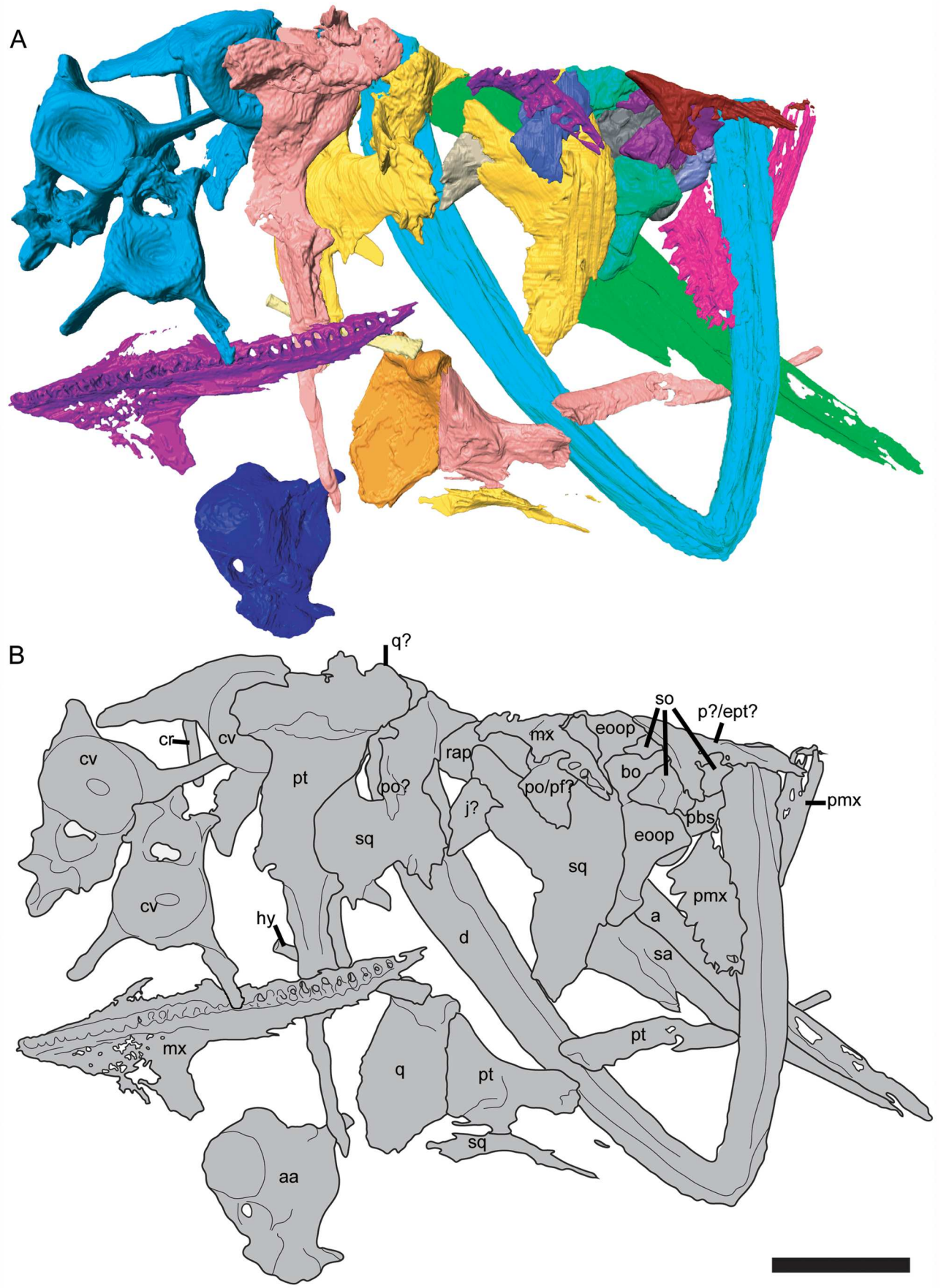

FIGURE 2. The segmented disarticulated skull and cervicals of EC K2134. **A**, segmented elements of side 1; **B**, interpretation of the elements. **Abbreviations**: **a**, angular; **aa**, atlas axis; **bo**, basioccipital; **cv**, cervical vertebra; **cr**, cervical rib; **d**, dentary; **ept?**, ectopterygoid?; **eoop**, exoccipital-opisthotic; **hy**, hyoid; **j?**, jugal?; **mx**, maxilla; **p**, parietal; **pbs**, parabasisphenoid; **pmx**, premaxilla; **po/pf?**, postorbital/postfrontal?; **pt**, pterygoid; **q**, quadrate; **rap**, retroarticular process; **sa**, surangular; **sq**, squamosal; **so**, supraoccipital. Scale bar equals 5 cm.

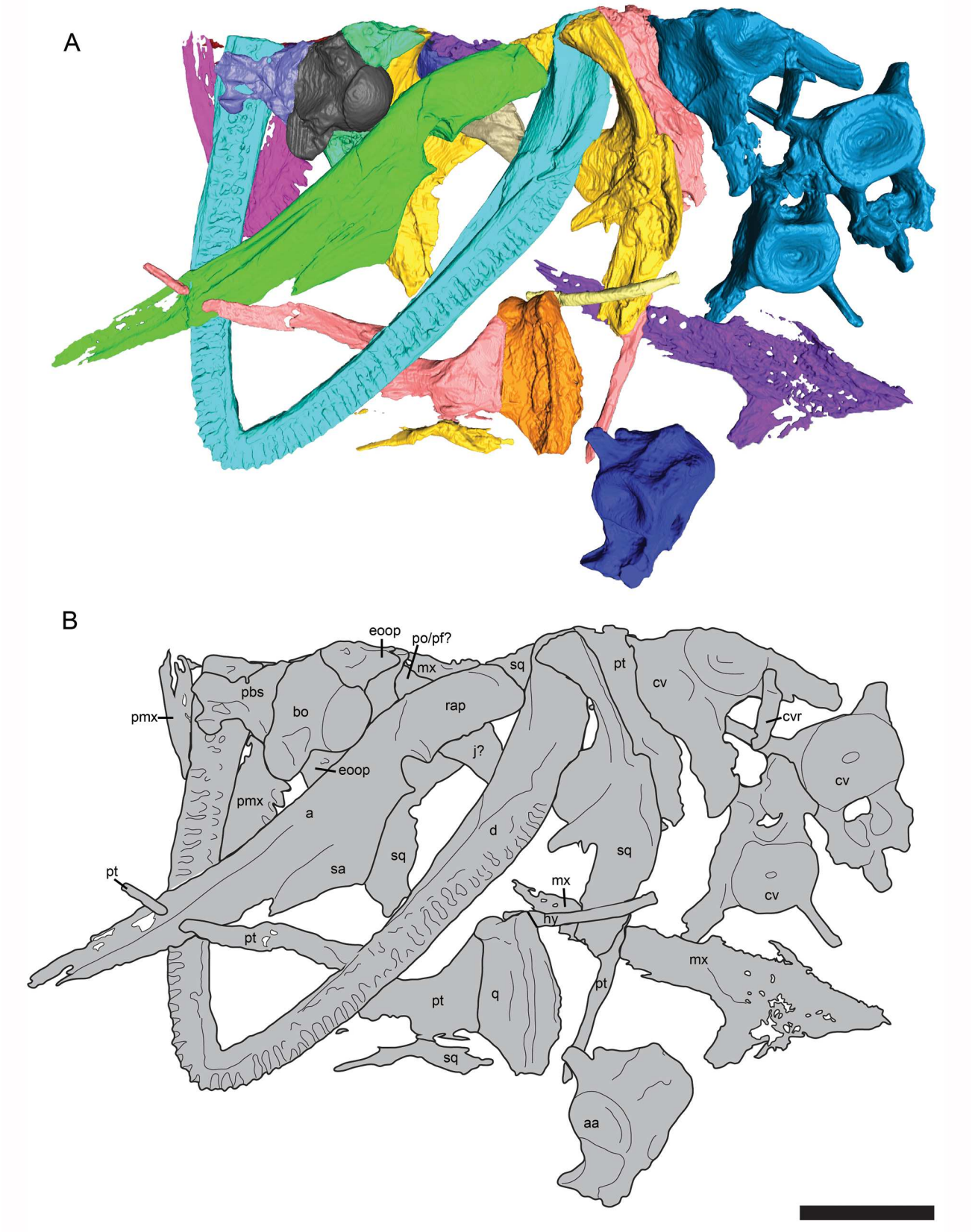

FIGURE 3. The segmented disarticulated skull and cervicals of EC K2134. **A**, segmented elements of side 2; **B**, interpretation of the elements. **Abbreviations**: **a**, angular; **aa**, atlas axis; **bo**, basioccipital; **cv**, cervical vertebra; **cvr**, cervical rib; **d**, dentary; **eoop**, exoccipital-opisthotic; **hy**, hyoid; **j?**, jugal?; **mx**, maxilla; **pbs**, parabasisphenoid; **pmx**, premaxilla; **po/pf?**, postorbital/postfrontal?; **pt**, pterygoid; **q**, quadrate; **rap**, retroarticular process; **sa**, surangular; **sq**, squamosal. Scale bar equals 5 cm.

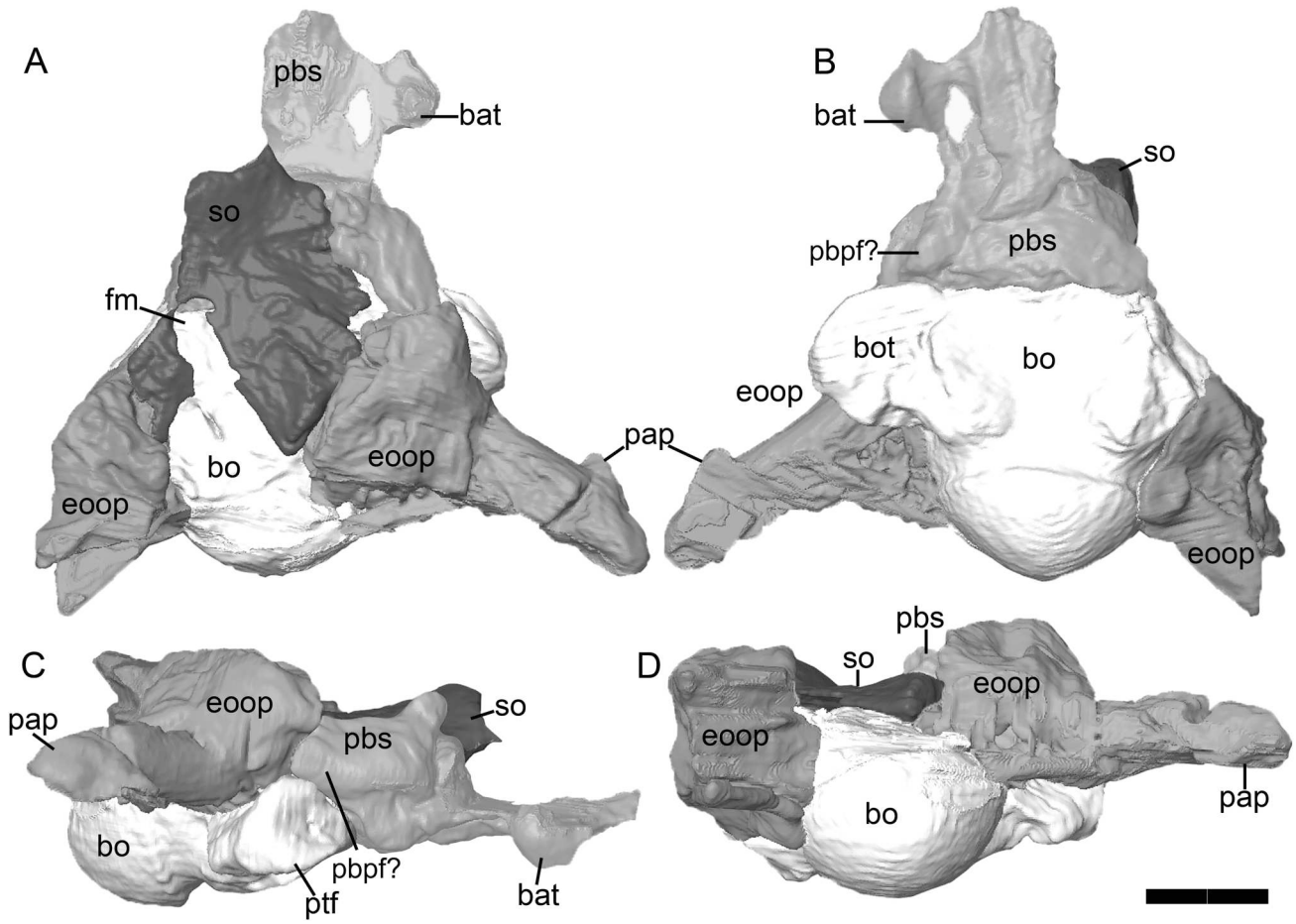

FIGURE 4. The segmented braincase of EC K2134. **A**, dorsal view; **B**, ventral view; **C**, lateral view; **D,** posterior view. **Abbreviations**: **bat**, basal articulation; **bo**, basioccipital; **bot**, basioccipital tubera; **eoop**, exoccipital-opisthotic; **fm**, foramen magnum; **pap**, paraoccipital process; **pbpf?**, possible parabasisphenoid pterygoid facet; **pbs**, parabasisphenoid; **ptf**, pterygoid facet; **so**, supraoccipital. Scale bar equals 5 cm.

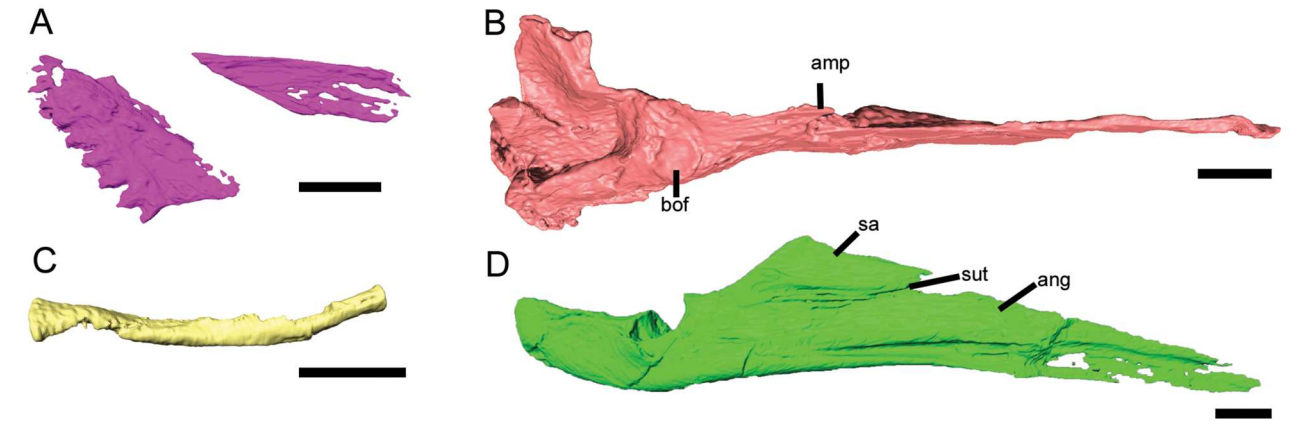

FIGURE 5. Selected segmented cranial and mandibular elements of EC K2134. **A**, left premaxilla in ventral view; **B**, left pterygoid in medial view; **C**, hyoid in medial/lateral view; **D**, posterior right mandible in lateral view. **Abbreviations**: **amp**, anteromedial process; **ang**, angular; **bof**, basioccipital facet; **sa**, surangular; **sut**, suture. Scale bars equal 2 cm.

M. leedsii (Andrews, 1910). Dentition is missing from this element.

Additional Skull Elements—There are several fragmented and disarticulated elements which represent different parts of the cranium in EC K2134. The two largest of these (Supplementary File 1, Fig. S2), represent the squamosals and some of the articulating elements. Both are significantly compressed, distorting their morphology. In lateral view, the suspensorium is vertically inclined, but slightly convex along the posterior margin. Dorsally, the squamosal curves anteromedially, with a robust post-temporal bar as in the holotype of *Kimmerosaurus langhami* (NHMUK R.8431). The anterior ramus is preserved on both sides with the ventral border of the anterior (lateral) ramus positioned dorsally to a level well above the quadrate condyle. This morphology is shared in the other specimens of *K. langhami*, *Cryptoclidus eurymerus*, *Tatenectes laramiensis*, *Tricleidus seelyei*, and *Muraneosaurus leedsii* (Andrews, 1910; Brown, 1981; Brown et al., 1986; O'Keefe & Wahl, 2003). However, in *Spitrasaurus larseni*, the ventral margin of the anterior ramus is in line with the quadrate condyle (Knutsen et al., 2012b). On the left squamosal an additional element likely representing part of the jugal is preserved in articulation. Based on the suture visible on the specimen (Supplementary File 1, Fig. S2B), the jugal articulates with postorbital anterodorsally, excluding the dorsal-most section from the orbital margin. This morphology is similar to that described for the referred specimen of *K. langhami* (NHMUK R.1798, Brown et al., 1986) and *C. eurymerus* (Brown & Cruickshank, 1994). A rectangular disarticulated element overlying the left squamosal, may represent the postorbital/postfrontal. This element has a distinct facet on one of the longer margins, which may represent a facet for the squamosal. On the right squamosal more of the postorbital bar is preserved, but significantly distorted and accurate separation of individual elements is not possible. Posteriorly, the ventromedial process with a medially facing facet for the quadrate is well-preserved. As in other specimens of *K. langhami*, this process is dorsoventrally elongated in comparison with the shorter process described in *Ophthalmothule cryostea* (Roberts et al., 2020). This morphology is similar in length, but more robust to that seen in *M. leedsii* and *C. eurymerus* (Andrews, 1910; Brown, 1981; Brown & Cruickshank, 1994). In posterior view, a slight depression is present just medial from the quadrate facet, which is likely for the paraoccipital process of the exoccipital-opisthotic.

A small element, representing either part of the skull roof or palate overlies the braincase. Being at the edge of the specimen, only part of this element is preserved. One end displays a section representing a large interdigitating suture. This element has a preserved rim for either the orbit or temporal fossa. As such, it is likely either part of a frontal, ectopterygoid, or parietal. Frontal is unlikely due to the short mediolateral width of the element. Dorsal ornamentation is commonly observed on parietals (Andrews, 1910) and is clearly present on the holotype of *Kimmerosaurus langhami* (Brown, 1981), but is largely missing on this element in EC K2134. As such, we tentatively identify this as part of the ectopterygoid.

Braincase—The braincase is almost entirely embedded in the matrix; however, the individual elements are deformed and overlying each other (Fig. 4). Of these elements, the basioccipital condyle is best preserved. A notochordal pit is absent on the occipital condyle in EC K2134 (Fig. 4D), as in referred specimen of *Kimmerosaurus langhami* NHMUK R1798 (Brown et al., 1986). This differs from the holotype specimen, where a notochordal pit is present (Brown, 1981). As in specimens of *K. langhami*, the condyle is clearly separated from the rest of the basioccipital with no true constriction or groove present (Brown et al., 1986). Similar to the referred specimen of *K. langhami* (NHMUK R.8431), the condyle is wider than it is tall with a height-to-width ratio of 0.6, significantly smaller than *Ophthalmothule cryostea* (0.82; Roberts et al., 2020), *Spitrasaurus larseni* (0.80; Knutsen et al., 2012b), and the type specimen of *K. langhami*, NHMUK R.8431 (0.85; Brown, 1981). It is unclear if the exoccipital-opisthotic contributes to the occipital condyle as in the type specimen (Brown, 1981), due to overlying elements compressing this area. Only the right basioccipital tuber is fully preserved but is compressed. Although compressed, it is similar to the pillar-like tubera of the described specimens of *K. langhami* (Brown et al., 1986), and bears a clear facet for the pterygoid. This differs from the dorsoventally flattened and triangular outline in *O. cryostea* (Roberts et al., 2020). Laterally, the tubera appear to have no or limited articulation to the basisphenoid, in contrast to *O. cryostea* where the tubera joins with the basisphenoid margin along its whole anteroposterior length (Roberts et al., 2020). Paired foramina are visible ventrally and move dorsally through the element. The ventral surface is flattened but lacks the anteroposteriorly ventral ridge present on the *K. langhami* holotype (Brown, 1981).

Part of the basisphenoid is articulated and partially fused to the basioccipital (Fig. 4A–C). This element appears anteroposteriorly short, although there is no clear border with the parasphenoid. This is a common feature in osteologically mature cryptoclidid specimens and has been observed in several cases (Roberts et al., 2020). As such, this element will be referred to as the "parabasisphenoid." The anterior margin of parabasisphenoid is damaged and may have extended into the interpterygoid vacuity. A lateral, bulbous extension forms the basal articulation to the pterygoid present on the right side. This morphology is shared with *Ophthalmothule cryostea* (Roberts et al., 2020), but differs from the mediolaterally shorter and anteroposteriorly longer basal articulation in *Tricleidus seeleyi* (Andrews, 1910). On the posterodorsal margin, bordering the basioccipital, a small depression is present. Although poorly preserved, this feature is likely to be the dorsal median pit. This structure is observed on the basioccipital of the type specimen of *Kimmerosaurus langhami* (NHMUK R. 8431) and the basisphenoid of *Muraenosaurus leedsii* and *O. cryostea* (Andrews, 1910; Brown, 1981; Roberts et al., 2020). In dorsal view, remains of a deep pituitary (or hypapophyseal) fossa is present as in all cryptoclidids where this element is preserved (Andrews, 1910; Roberts et al., 2020). In ventral and lateral view, a facet for the pterygoid appears present posterolaterally as in *O. cryostea* and *T. seeleyi* but contrasting to *Cryptoclidus eurymerus* where this is absent (Andrews, 1910; Brown, 1981; Roberts et al., 2020). This feature was also suggested present on the referred specimen of *Kimmerosaurus langhami* (NHMUK R10042, Benson & Druckenmiller, 2014). However, in EC K2134 this region is significantly damaged from the overlying dentary. It should be mentioned that only a short and partial anteromedial process of the pterygoid was preserved in EC K2134, unlike the extended process seen in *O. cryostea* and *T. seeleyi* (Andrews, 1910; Roberts et al., 2020). As the presence of a facet on the parabasisphenoid suggests, if a longer anteromedial process of the pterygoid is present in EC K2134, then this process is either missing or not ossified.

The exoccipital-opisthotics are articulated to the basioccipital, although the left is missing the paraoccipital process (Fig. 4). As such, the right exoccipital-opisthotic will largely be used for the description. Both elements are dorsoventrally compressed, so some aspects of their morphology are difficult to interpret. In lateral view, several foramina are visible close to the facet with the basioccipital. The largest of these is likely to belong to cranial nerve X, as in the holotype of *Kimmerosaurus langhami* and *Ophthalothule cryostea* (Brown, 1981; Roberts et al., 2020). The paraoccipital process is longer than the total height of the element; however, this is likely exaggerated due to the compression of the element. As in *O. cryostea* (Roberts et al.,

2020), *Cryptocleidus eurymerus* (Andrews, 1910), and the holotype of *K. langhami* (Brown, 1981), the paraoccipital process is expanded distally to contact the squamosal. The process itself, although slightly crushed, closely resembles the robust process seen in *K. langhami*, contrasting to the more robust process observed in Oxford Clay cryptoclidids (Andrews, 1910; Brown, 1981). On the medial surface, a horizontal groove is present, which may represent either the horizontal semicircular canal or fenestra ovalis (Brown, 1981).

The right half of the supraoccipital is completely preserved, on top of the basioccipital and parabasisphenoid (Fig. 4A). The element preserves the lateral process articulating to exoccipital-opisthotics and a dorsal facet for the parietal/squamosal. The supraoccipital is too damaged to identify a posteromedian ridge which is present in a specimen of *Kimmerosaurus langhami* (Brown et al., 1986, NHMUK R10042). Based on the preserved parts of the element, the foramen magnum of EC K2134 was dorsoventrally taller than mediolaterally wide.

Pterygoid—Both pterygoids are preserved (Figs. 2, 3). Although nearly complete, the left pterygoid is posteriorly fused to parts of the left quadrate and squamosal, making segmentation of the posterior region challenging. It has been medio-laterally compressed so the extension which connects with the palatine appears distorted. The right pterygoid is broken into several pieces, where the posterior portion is fused to the left quadrate. As such the left pterygoid will be the focus of the description.

Although exaggerated by taphonomy, the general morphology of the pterygoid is mediolaterally narrow anteriorly and increasing in mediolateral width posteriorly similar to *Cryptoclidus eurymerus*, *Muraneosaurus leedsii*, and *Ophthalmothule cryostea* (Andrews, 1910; Brown, 1981; Brown & Cruickshank, 1994, Roberts et al., 2020). Anteriorly the pterygoid is thickened to contact the vomer, although this element is missing in EC K2134. Based on the mediolateral extensions of both pterygoids, likely a broad anterior interpterygoid fenestra separated the two elements, a feature common in many cryptoclidids (e.g., *O. cryostea*, Roberts et al., 2020), but can be narrow in some (e.g., *M. leedsii*: Andrews, 1910; Brown, 1981). The pterygoid forms the lateral margin of the posterior interpterygoid vacuity, based on the morphology of the medial margin of the pterygoid. Similar to *O. cryostea* and *Tricleidus seeleyi*, the posterior interpterygoid vacuity is positioned posteriorly inline to the anterior margin of the subtemporal fossa (Roberts et al., 2020). However, the size of the posterior interpterygoid vacuities appear to be significantly limited in width based on the articulation of the pterygoid with the basioccipital. A short but anteroposteriorly extended anteromedial process is present, which likely reached the parabasisphenoid. With the presence of a clear facet on the parabasisphenoid, it is now possible to confirm the previously suggested morphology of an anteromedial process of the pterygoid in *Kimmerosaurus langhami* (Benson & Druckenmiller, 2014; Roberts et al., 2020). This anteromedial process is partially broken and appears shorter than that observed in *T. seeleyi* and *O. cryostea* (Andrews, 1910; Roberts et al., 2020).

Dorsomedially, on the posterior region of the pterygoid, a clear facet for the basioccipital tubera is visible on both pterygoids (Fig. 5B). This is similar, if not identical to the morphology of the type specimen of *Kimmerosaurus langhami* (NHMUK R.8431, Brown, 1981).

Posteriorly, the pterygoids are fused to the quadrate and part of the squamosal overlays and distorts this region on the left side. On the right side, a suture was visible using the CT images, allowing for separate segmentation of these regions (Supplementary File 1, Fig. S2C). Although partly damaged dorsally, the quadrate facet on the right pterygoid is large and restricted to the lateral edge of the pterygoid as in the holotype of *Kimmerosaurus langhami* (NHMUK R.8431, Brown, 1981). This differs from *Tricleidus seeleyi* and *Muraenosaurus leedsii*, where the posterior end of the pterygoid articulated in an anterolateral notch in the quadrate (Brown, 1981).

Quadrate—The right quadrate is complete, whereas only part of the left quadrate is preserved compressed onto the dorsal region of the pterygoid. On the right quadrate, part of the pterygoid and possibly some parts of the squamosal are fused to the quadrate (Supplementary File 1, Fig. S2C).

Dorsally and laterally a rugose surface is present for the articulation to the squamosal, consisting of a deep dorsoventrally orientated groove laterally, with additional ridges anterolaterally. These terminate ventrally at the quadrate condyle. The lateral condyle is subtly larger than the medial condyle, although not to the same degree as in the *Kimmerosaurus langhami* type specimen (NHMUK R.8431, Brown, 1981) and other Tithonian cryptoclidids (*Djupedalia engeri* and *Ophthalmothule cryostea,* Knutsen et al., 2012c; Roberts et al., 2020). This differs from *Spitrasaurus larseni*, which has a significantly larger medial condyle, than lateral condyle (Knutsen et al., 2012b). Similar to the type specimen of *K. langhami*, the pterygoid facet appears to be vertically orientated based on the fragment of the pterygoid articulated to the element (Brown, 1981).

Mandible—*Kimmerosaurus langhami* is noted for its large number of teeth and as with the holotype (NHMUK R.8431, Brown, 1981), the dentary of EC K2134 is estimated to preserve 36 alveoli (Fig. 2). The sockets suggest the teeth were labially angled almost horizontal from the parasagittal plane, and likely, as in the holotype (NHMUK R.8431, Brown, 1981), held markedly recurved teeth similar to *Spitrasaurus larseni* and *Ophthalmothule cryostea* (Knutsen et al., 2012b; Roberts et al., 2020). Specimen EC K2134 unfortunately completely lacks dentition. As in the holotype for *Kimmerosaurus langhami* (NHMUK R.8431), there is limited mediolateral expansion of the dentary; however, the feature was noted present in the referred specimen of *K. langhami* (NHMUK R.10042) by Roberts et al. (2020). In EC K.2134, a limited mediolateral expansion of the dentary is only present in the posterior third of the dentary, similar to *Cryptoclidus eurymerus* (Andrews, 1910).

The posterior lower right mandible has become disarticulated from the lower jaw and is preserved in its entirety (Fig. 5D). There is little lateral curvature in these elements except where it intersects with the dorsal surface of the right ramus, here a groove has been imposed onto the angular lateral surface. The mandibular glenoid, which attaches with the quadrate, is well preserved and is relatively shallow: the depth contributing about a quarter of the mandibular height (half the mandibular height in *Ophthalmothule cryostea*, Roberts et al., 2020). The surface of the glenoid is smooth, much like *Cryptoclidus eurymerus* and *Muraenosaurus leedsii* (Brown, 1981). There is a ridge running anteroposteriorly along the lingual side of the right angular, likely articulation for the splenial. Ventral to the glenoid, the ventral margin of the angular is convex as in the type specimen of *K. langhami* and *C. eurymerus.* In contrast, this margin is relatively straight in *O. cryostea* and *Tricleidus seeleyi* (Andrews, 1910; Roberts et al., 2020).

The retroarticular process is dorsally inclined at 27°, equal to the *Colymbosaurus* Oxford specimen (OUM J.3300) and slightly larger than the type specimen of *Kimmerosaurus langhami* ~21° (Roberts et al., 2017, 2020). These are all larger than the inclination in *Ophthalmothule cryostea* (PMO 224.248; ~15°, Roberts et al., 2020) and *Tricleidus seeleyi* (10°, Brown, 1981), but smaller than *Spitrasaurus larseni* (35°, Knutsen et al., 2012b). The retroarticular process is almost twice as long as it is tall, similar to that of *O. cryostea* and the type specimen NHMUK R. 8431 (Roberts et al., 2020; Brown, 1981). There is no mediolateral deflection.

Hyoid—A single hyoid is preserved as a complete element, although compressed due to overlying material (Fig. 5C). This is the first to be described from a cryptoclidid plesiosaur. Although other possible specimens are known to be present in other specimens from the Oxford Clay Formation but are currently undescribed (M. Evans personal communication, September 21, 2023). The element is roughly oval in cross section and terminates at a broader, flatter end. This is easily distinguishable from a cervical rib, as these are anteroposteriorly broad and flat and are mediolaterally thin in cross section. One end is flattened, whereas the other displays a circular facet. The element displays some curvature and is oval in cross section at the midshaft.

Axial Skeleton

There are six cervical vertebrae in the specimen including the atlas–axis, three grouped to the left of the lower jaw at the edge of the block and an additional cervical not included in the CT scan (Fig. 1). Of the three cervicals (not including atlas–axis) present in the scan, their size and location within the block suggest that they are all consecutive cervical vertebrae. In these anterior cervicals, the neural arch is fused to the cervical centrum, implying that this specimen is an adult (Brown, 1981).

Atlas–Axis—The atlas–axis complex is completely fused; however, there is a discernible suture laterally but difficult to trace dorsally at the base of the neural arch (Fig. 6A–C). This morphology reflects the advanced ontogenetic status of EC K2134. The complex is slightly wider than it is long with a width/length ratio of 1.3, similar to *Spitrasaurus larseni* and *Colymbosaurus megadeirus* (Benson & Bowdler, 2014; Knutsen et al., 2012b), unlike *Opthalmothule cryostea* and *Muraenosaurus leedsii* where the complex is approximately twice as long as it is wide (Andrews, 1910; Roberts et al., 2020).

In anterior view, the atlantal cup covers the entire width and height of the centrum body. It is circular, unlike the oval morphology of the referred *Kimmerosaurus langhami* material (NHMUK R.10042; Brown et al., 1986). Although it should be mentioned that NHMUK R.10042 has suffered some mediolateral taphonomic compression, as suggested by Benson and Bowdler (2014). Like the referred material, however, the centrum is strongly concave and bears a resemblance to the atlas–axis complex of *Cryptoclidus eurymerus* (NHMUK R2869; Andrews, 1910; Brown et al., 1986). Ventrally, the hypapophyseal eminence is present on the ventral surface of the element, reaching just posterior to the atlas–axis suture. This feature is more posteriorly positioned compared with *Opthalmothule cryostea* and *Colymbosaurus megadeirus* (Benson & Bowdler, 2014; Roberts et al., 2020). In NHMUK R.10042, *Tatenectes laramiensis*, '*Plesiosaurus*' *manselii* (NHMUK PV OR 42496), *Cryptoclidus eurymerus* (NHMUK R.2860), and *Muraenosaurus leedsii*, the hypapophyseal eminence extends further onto the axis centrum (Andrews, 1910; Benson & Bowdler, 2014; Brown et al., 1986; O'Keefe & Wahl, 2003). However, in the case of the NHMUK R.10042, as previously noted this is likely due to the taphonomic distortion of the element. The atlas–axis neural arch is preserved in a similar state to NHMUK R.10042 and lacks almost all ornamentation. The neural arches of the atlas–axis complex are fused together and bear a short, posteriorly angled neural spine. The axial postzygopophyses are separate from the neural spine as in *Cryptoclidus eurymerus* (NHMUK R.2860; Andrews, 1910). As in most cryptoclidids, atlantal ribs are present and fully preserved on the right side (Andrews, 1910; O'Keefe & Wahl, 2003). The exception here being *C. megadeirus*, which lacks atlantal ribs (Benson & Bowdler, 2014). A character which has significantly assisted in separating *Kimmerosaurus langhami* and *C. megadeirus* (Benson & Bowdler, 2014). The axial rib spans most of the axis length, similar to *O. cryostea* and NHMUK R.10042 (Roberts et al., 2020; Brown et al., 1986). This is dissimilar to the elongated axial ribs seen in *C. eurymerus* (NHMUK R.2860, Andrews, 1910).

Anterior Cervical Vertebrae—The anterior cervicals (Fig. 6D, E) are all mediolaterally wider than they are anteroposteriorly long, as in *Cryptoclidus eurymerus, Ophalthothule cryostea* and the referred material of *Kimmerosaurus langhami* (Andrews, 1910; NHMUK R.10042, Brown et al., 1986; Roberts et al. 2020). As in *K. langhami* (NHMUK R.10042), *Djupedalia engeri*, and *Colymbosaurus*, all of the cervicals of EC K2134 have circular, strongly amphicoelous centra (Knutsen et al. 2012c; Brown et al., 1986). Other cryptoclidid plesiosaurs display weakly concave to flat articular surfaces: *Opallionectes andamookaensis* (shallowly amphicoelous to platycoelous; Kear, 2006), *Spitrasaurus wensaasi* (platycoelous, Knutsen et al., 2012b), *Spitrasaurus larseni* (platycoelous to near flat; Knutsen et al., 2012b), *Abyssosaurus nataliae* (platycoelous; Berezin, 2011) and *Muraenosaurus leedsii* (platycoelous; Andrews, 1910). As in the *K. langhami* specimen NHMUK R.10042, the centra have convex rims on the articular surface, giving a double sigmoid curve in cross-section (Brown et al., 1986). The vertebrae lack lateral ridges on the cervical centrum contrasting to

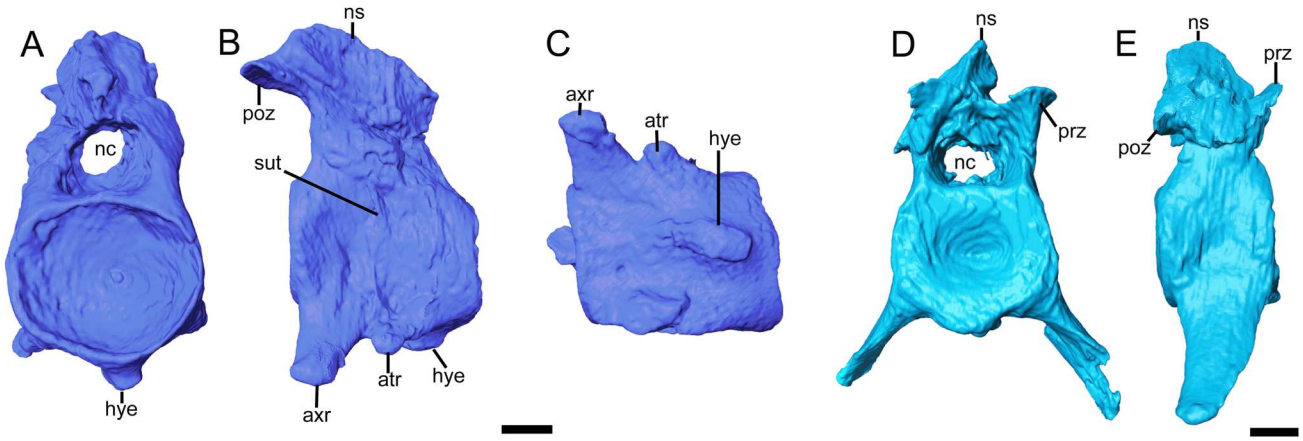

FIGURE 6. Selected segmented elements of the axial skeleton of EC K2134. **A**, atlas–axis in anterior view; **B**, atlas–axis in lateral view; **C**, atlas–axis in ventral view; **D**, cervical vertebrae in anterior view; **E**, cervical vertebrae in lateral view. **Abbreviations**: **atr**, atlantal rib; **axr**, axial rib; **hye**, hypapophyseal eminence; **nc**, neural canal; **ns**, neural spine; **poz**, postzygopophysis; **prz**, prezygopophysis; **sut**, suture. Scale bars equal 1 cm.

Spitrasaurus spp. and *M. leedsii*, where these are present (Brown, 1981; Knutsen et al., 2012b). Similar to *M. leedsii*, *D. engeri*, *O. cryostea* and NHMUK R. 10042, the lateral surfaces of the centra are all concave (Andrews, 1910; Knutsen et al., 2012c; Roberts et al., 2020). There is a small bulge on the ventral surface of one of the vertebrae, but this is absent from the rest. This seems more to be pathological in nature, as it does not resemble the anteroposteriorly long ventral keel in *O. cryostea* and *Tricleidus seeleyi* (Andrews, 1910; Roberts et al., 2020). Subcentral foramina are widely spaced, similar to *O. cryostea* (Roberts et al., 2020).

The cervical ribs are fused ventrolaterally to the centrum, these are narrow in anterior view and single headed as in the referred material (Brown et al., 1986). In lateral view, they take a broad, flat shape, with a width equal to the whole centrum (Fig. 6E). They extend straight down with no curvature as in the referred specimen of *Kimmerosaurus langhami* (NHMUK R. 10042, Brown et al., 1986). This differs from the slight posterior curvature in *Spitrasaurus wensaasi* and the extreme posterior curvature in *Ophthalmothule cryostea* (Knutsen et al., 2012b; Roberts et al., 2020). There are no anterior projections on the cervical ribs in EC K2134, as in Oxford Clay Formation cryptoclidids (Andrews, 1910; Brown, 1981).

The neural spine extends dorsally as straight processes directly above the centrum, similar to the referred material of *Kimmerosaurus langhami* (NHMUK R.10042, Brown et al., 1986) and in *Colymbosaurus megadeirus* (Benson & Bowdler, 2014; Brown, 1981). This differs from *Ophthalmothule cryostea* where they are angled posteriorly (Roberts et al., 2020) and *Spitrasaurus* spp., *Muraenosaurus leedsii*, *Cryptoclidus eurymerus*, and *Tricleidus seeleyi*, where the neural spines are posteriorly shifted (Andrews, 1910; Brown, 1981; Knutsen et al., 2012b). The neural spine is similar in general morphology as in the referred material (Brown et al., 1986). Dorsal to the postzygapophyses an anteroposterior ridge runs up the neural spine, a feature also observed in *K. langhami* (NHMUK R.10042). This structure is also present in *Cryptoclidus eurymerus* and *Muraenosaurus leedsii* (Brown et al., 1986). As described for NHMUK R.10042, *C. eurymerus*, the pre- and postzygapophyses are separated along their entire length. This differs from *Spitrasaurus* spp. where both are fused throughout the cervical series (Knutsen et al., 2012b). In *O. cryostea*, the prezygapophyses are separate in anterior cervicals, but the postzygapophyses are fused (Roberts et al., 2020). In *Djupedalia engeri*, the prezygapophyses are fused, whereas the postzygapophyses are separate in anterior cervicals (Knutsen et al., 2012c).

DISCUSSION

Phylogenetic Position

The phylogenetic result is displayed for Cryptoclididae in Figure 7, with time constraints utilized from Roberts et al. (2020). The analysis resulted in a total of 576 MPTs (most parsimonious trees), with a best score of 1328. The consistency index (CI) was 0.297 and the retention index (RI) was 0.664. The full strict consensus tree is available in Supplementary File 1 (Fig. S3), and all MPTs are presented in Supplementary File 2. Bootstrap replication results are displayed in Figure S4. The phylogenetic analysis shows EC K2134 nested in a polytomy alongside *Kimmerosaurus langhami* and *Tatenectes laramiensis*. There is limited overlapping material between *K. langhami* + ECK2134 and *T. laramiensis*, which has likely been the cause of the inability to resolve this clade. The presence of the polytomy involving *K. langhami* and EC K2134, further supports the referral of EC K2134 to *K. langhami*, as the differences between the scoring of these two OTUs is minimal. This is a reflection of the different scorings for a specific character on the atlas–axis (146) and cervical vertebral dimensions (153). However, the previously described atlas–axis material for *K. langhami*, has suffered some taphonomic distortion and this might explain some of the observed differences. Few differences are present between this analysis and the analysis completed by Roberts et al. (2020). In our analysis, the position of *Cryptoclidus eurymerus* has moved from its original position as sister taxon to *K. langhami* + *T. laramiensis*, to a more basal position in the tree.

New Information on *Kimmerosaurus langhami*

There are only three described specimens of *Kimmerosaurus langhami* and so this taxon, like many other cryptoclidids, suffers from a lack of referred material. However, additional material remains identified (Stokke, 2022) and is currently under study in the PMO collection from the Tithonian of Svalbard. The initial description on the type specimen (NHMUK R.8431) by Brown (1981) provided details on the frontal, parietal, part of the squamosal, quadrate, basioccipital, postorbital, postfrontal, exoccipital-opisthotic, mandible, and dentition (11 teeth). Further referred material (NHMUK R.1798, NHMUK R.10042) described by Brown et al. (1986) includes five vertebrae, posterior left mandible fused with a portion of the dentary, the basioccipital, both exoccipital-opisthotics, the basisphenoid and the supraoccipital. Specimen EC K2134 adds to our knowledge of the skull morphology of *K. langhami*, the rostral morphology, postorbital bar, posterior palate and number of teeth. One of the main findings from EC K2134 is the morphology of the basicranium for *K. langhami*, which previously has only been hypothesized (Benson & Druckenmiller, 2014; Roberts et al., 2020). Our study confirms a strong basal articulation as well as short anteromedial process of the pterygoid. Adding EC K2134 to *K. langhami* enables adds to the cranial reconstruction for the taxon (Fig. 8), based on Brown (1981) and Brown et al. (1986).

Differences Between the Holotype and Referred Specimens of *Kimmerosaurus langhami* and EC K2134

There are several differences in the morphology of the atlas–axis, basioccipital, quadrate, and mandible when compared with type specimen and previously referred material of *Kimmerosaurus langhami*. The basioccipital condyle height to width ratio of EC K2134 is 0.6, significantly smaller than the 0.85 ratio in the type specimen. EC K2134 does not clearly display the participation of the exoccipital pedicels in the occipital condyle seen on the holotype. However, this morphology is also shared with the referred specimen NHMUK R.1798. The ventral surface of the basioccipital lacks anteroposteriorly oriented ventral ridge present on the holotype of *K. langhami*. We suggest that at least to the differences in morphology of the extent of the exoccipitals, may depend on ontogeny and exoccipital contribution to the occipital condyle may not be visible in older individuals such as NHMUK R.1798 and EC 2134.

In EC 2134, the lateral condyle of the quadrate is subtly larger than the medial condyle but clearly not to the same degree as the type specimen NHMUK R.8431. The retroarticular process of the mandible is inclined at 27°, slightly larger than the type specimen at ~21°. This subtle difference is minor when compared with the variability of the state in other taxa of cryptoclidids (e.g., *Spitrasaurus* spp.; Knutsen et al., 2012b). In NHMUK R.10042, the lateral surfaces of the atlas–axis centra are significantly more concave than EC K2134. We agree with Benson and Bowdler (2014), that the mediolaterally compressed atlas–axis in the *Kimmerosaurus langhami* specimen NHMUK R.10042 is likely the source of the differences between EC K2134 and NHMUK R.10042. We assume that the morphology of hypapophyseal

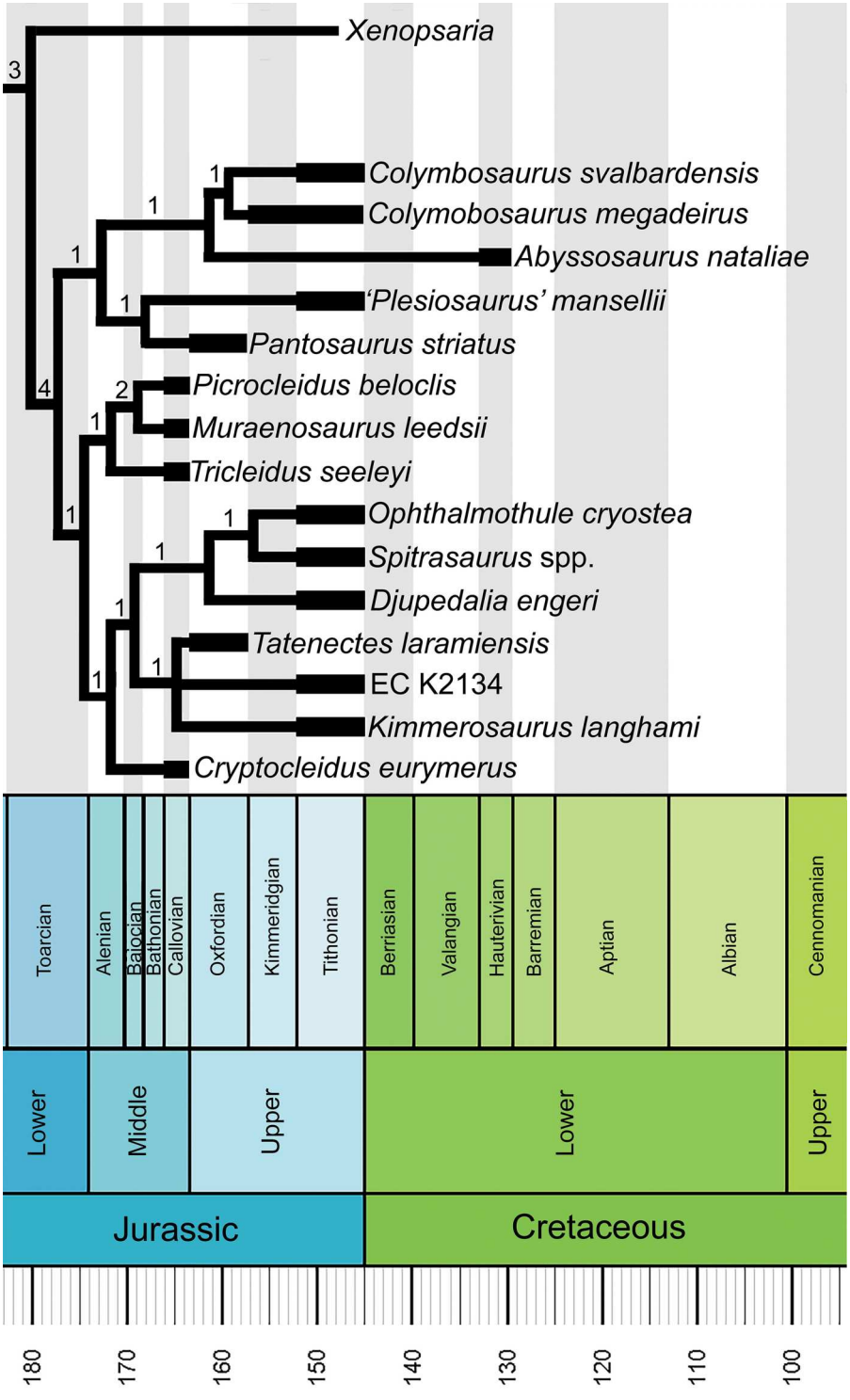

FIGURE 7. Reduced phylogenetic tree of Cryptoclididae with time constraints using range data from Roberts et al. (2020). Bremer supports displayed over the branches.

eminence of EC K2134 bears a more accurate representative morphology for the taxon.

Hyoids in Plesiosauria and Future Implications

Although rare in the plesiosaur fossil record, a few hyoid elements have been described from other plesiosaur specimens and likely derive from ceratobranchical 1 as in other Mesozoic marine reptiles (Delsett et al., 2023). Plesiosaur specimens with hyoids include the basally branching plesiosaur *Stratesaurus taylori* (Benson et al., 2015), elasmosaurids (Kear, 2005; Marx et al., 2021; Serratos et al., 2017), polycotylids (Druckenmiller, 2002; Schumacher & Martin, 2015), pliosaurids (O'Gorman et al., 2018; Páramo-Fonseca et al., 2018, 2019; Storrs & Taylor, 1996; Vincent, 2011) and rhomalosaurids (Smith & Vincent, 2010; Taylor, 1992). EC K2134 represents the first cryptoclidid for which this is described. As the hyoid apparatus is considered a crucial component in feeding in marine tetrapods, the

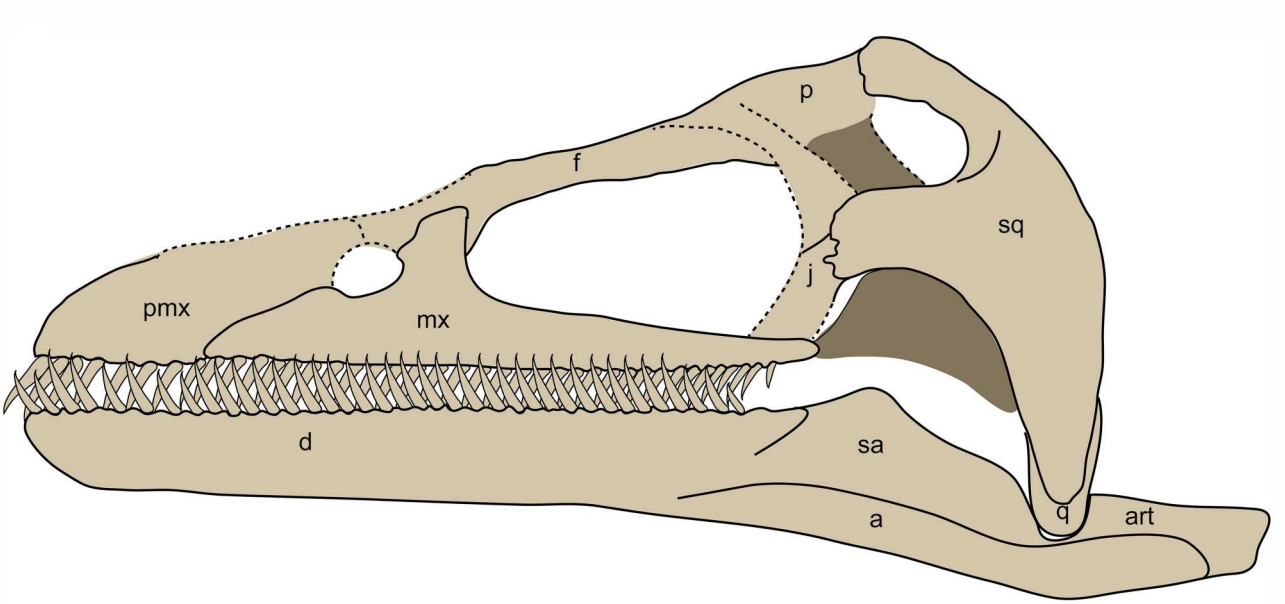

FIGURE 8. New lateral reconstruction of the cranium of *Kimmerosaurus langhami*, based on initial reconstructions by Brown (1981) and Brown et al. (1986). **Abbreviations: a**, angular; **art**, articular; **d**, dentary; **f**, frontal; **j**, jugal; **mx**, maxilla; **p**, parietal; **pmx**, premaxilla; **q**, quadrate; **sa**, surangular; **sq**, squamosal.

morphology of this element is likely to vary depending on prey type and feeding mode (Delsett et al., 2023). Comparing between pliosauromorph and plesiosauromorph hyoids, there appear to be distinct differences in morphology which may be linked to differences in cranial morphology and feeding mode.

Although rarely preserved in completion, hyoids in pliosauromorphs are usually gracile with slight curvature (Druckenmiller, 2002; Storrs & Taylor, 1996) and are generally shorter in comparison to total length. In the pliosaurid *Eardasaurus powelli* the hyoid represents roughly 17% of total skull length (Ketchum & Benson, 2022). In a larger pliosaurid, *Stenorhynchosaurus munozi,* the complete hyoid represents 21% of total skull length (Páramo-Fonseca et al., 2019).

In comparison, hyoids from plesiosauromorph taxa are largely limited to Elasmosauridae, with the addition of this paper for Cryptoclididae. In the elasmosaurid *Nakonanectes bradti*, the hyoids are sigmoidal elements with anterior and posteriorly convex ends. In cross section this element varies from rectangular anteriorly to lunate posteriorly (Serratos et al., 2017). This is similar in EC K2134, although the hyoid is likely only curved and not sigmoidal due to crushing. The length of the hyoids in relation to cranium length in *N. brandti* is 23% (7.5 cm hyoid length/33 cm total skull length). The hyoid length to skull length ratio is similar in EC K2134, where the hyoids are approximately ~20% of total skull length. The partially preserved hyoids of the elasmosaurids *Cardiocorax mukulu* (Marx et al., 2021) and complete hyoids in *Eromangasaurus australis* (Kear, 2005, Sachs, 2005) differ from *N. bradti* by being nearly straight and rod-like and hyoid length is approximately around a third of the total skull length. At a glance the hyoid length/skull length relationship may be similar to that described for ichthyosaurs; where the length of hyoids shows a negative allometry with mandible length (Delsett et al., 2023). Although not as well-described in Plesiosauria, additional specimens described in recent years over multiple taxonomic groups suggest that a larger comparative study of hyoid morphology in Plesiosauria may now be possible.

CONCLUSION

In this paper we add more cranial and cervical material to the poorly known taxon *Kimmerosaurus langhami* from the Upper Jurassic Kimmeridge Clay Formation (U.K.). Specimen EC K2134 adds significant data regarding the palate, braincase, and dorsal skull elements of the taxon, as well as adding the first instance of hyoids described for Cryptoclididae. This has allowed us to increase the detail on the skull reconstruction of *Kimmerosaurus langhami* by Brown (1981) (Fig. 8). Due to the nature of disarticulation of the skull elements in EC K2134, some aspects of the relationships between individual elements remain unclear. The complete digital segmentation of this specimen has allowed for individual renderings of each element, allowing for 3D printing. This increases the accessibility of the specimen and allows it not only to be used for research, but also for educational purposes.

ACKNOWLEDGMENTS

Thank you to the reviewers which improved the quality of the manuscript. We are sincerely grateful to the staff at the μ-VIS X-Ray Imaging Centre, University of Southampton and the University of Bristol for scanning the block and for providing assistance and the means to conduct the technical aspect of this study. The authors wish to thank the museum curators and researchers that assisted AJR during collection visits to examine the comparative material; S. Chapman and L. Steel (NHMUK), M. Riley (CAMSM), E. Howlett (OUM), M. Evans (LEICS), M. Fernández (MOZ, MLP), G. Wass (PETMG), N. Clark (GLAHM), G. Cuny (MGUH), K. Sherburn (MANCH), L.A. Vietti (UW). E. Martin-Silverstone, P. S. Druckenmiller, E. M. Knutsen, M. Evans and D. Foffa are thanked for discussion. A. Hall is thanked for photographic assistance. The Willi Hennig Society are thanked for making TNT freely available.

AUTHOR CONTRIBUTIONS

SE, IH, JEAM, and NG created the initial project idea. SE collected, prepared, and completed initial identification of the specimen. KR completed the CT scanning of specimen and wrote the corresponding methods section of the manuscript. AJR and NH completed Avizo segmentation and interpretation of results. AJR and NH collected data for the phylogenetic analysis run by AJR. AJR and NH wrote the initial manuscript, with edits and additions from all other authors.

DATA AVAILABILITY STATEMENT

All data necessary to replicate the findings of the study are available in the paper or its supplemental information. Phylogenetic and measurement data used in this publication are available in the Supplementary Files. Due to consequences from the Covid epidemic, the original scan of the specimen was lost. However, segmentation work and interpretation were completed on the down-sampled dataset only. The down-sampled raw data tiff-stack, as well as the segmented models are available on Morphosource (https://doi.org/10.17602/M2/M594414). The phylogenetic dataset is available for download at MorphoBank (http://morphobank.org/permalink/?P5825).

DISCLOSURE STATEMENT

No potential conflict of interest was reported by the author(s).

SUPPLEMENTARY FILES

Supplementary File 1. Includes additional figures, tables and changes in character scoring for *Kimmerosaurus langhami* from Roberts et al. (2020).

Supplementary File 2. MPTs from the phylogenetic analysis.

ORCID

Aubrey J. Roberts http://orcid.org/0000-0003-2714-666X
Kathryn Rankin http://orcid.org/0000-0002-8458-1038

LITERATURE CITED

Andrews, C. W. (1910). *A Descriptive Catalogue of the Marine Reptiles of The Oxford Clay Based on the Leeds Collection in the British Museum (Natural History), London, Part I*. British Museum (Natural History).

Arkhangelsky, M. S., Zverkov, N. G., Rogov, M. A., Stenshin, I. M., & Baykina, E. M. (2020). Colymbosaurines from the Upper Jurassic of European Russia and their implication for palaeobiogeography of marine reptiles. *Palaeobiodiversity and Palaeoenvironments*, *100*(1), 197–218. https://doi.org/10.1007/s12549-019-00397-0

Bakker, R. T. (1993). Plesiosaur extinction cycles—events that mark the beginning, middle and end of the Cretaceous. *Special Papers of the Geological Association of Canada*, *39*, 641–664.

Benson, R. B. J., & Bowdler, T. (2014). Anatomy of *Colymbosaurus megadeirus* (Reptilia, Plesiosauria) from the Kimmeridge Clay Formation of the U.K., and high diversity among Late Jurassic plesiosauroids. *Journal of Vertebrate Paleontology*, *34*(5), 1053–1071. https://doi.org/10.1080/02724634.2014.850087

Benson, R. B. J., & Druckenmiller, P. S. (2014). Faunal turnover of marine tetrapods of the Jurassic–Cretaceous transition. *Biological Reviews*, *89*(1), 1–23. https://doi.org/10.1111/brv.12038

Benson R. B. J, Evans M. & Druckenmiller P. S. (2012). High diversity, low disparity and small body size in plesiosaurs (Reptilia, Sauropterygia) from the Triassic–Jurassic boundary. *PLoS ONE* *7*(3), e31838. https://doi.org/10.1371/journal.pone.0031838

Benson, R. B. J., Evans, M., & Taylor, M. A. (2015). The anatomy of *Stratesaurus* (Reptilia, Plesiosauria) from the lowermost Jurassic of Somerset, United Kingdom. *Journal of Vertebrate Paleontology*, *35*(4), https://doi.org/10.1080/02724634.2014.933739

Berezin, A. Y. (2011). A new plesiosaur of the family Aristonectidae from the Early Cretaceous of the center of the Russian platform. *Paleontological Journal*, *45*(6), 648–660. https://doi.org/10.1134/S0031030111060037

Blainville, H. D. d. (1835). Description de quel ques espèces de reptiles de la Californie, précédé de l'analyse d'un système général d'Erpétologie et d'Amphibiologie. *Nouvelles Annales du Museum National d'Histoire Naturelle, Paris*, *4*, 233–296.

Brown, D. S. (1981). The English Upper Jurassic Plesiosauridae (Reptilia)and a review of the phylogeny and classification of the Plesiosauria. *Bulletin of the British Museum (Natural History), Geology*, *35*(5), 253–347.

Brown, D. S., & Cruickshank, A. R. I. (1994). The skull of the Callovian plesiosaur *Cryptoclidus eurymerus*, and the sauropterygian cheek. *Palaeontology*, *37*(4), 941–953.

Brown, D. S., Milner, A. C., & Taylor, M. A. (1986). New material of the plesiosaur *Kimmerosaurus langhami* Brown from the Kimmeridge Clay of Dorset. *Bulletin of the British Museum (Natural History), Geology*, *40*(5), 225–234.

Delsett, L. L., Pyenson, N., Miedema, F., & Hammer, Ø. (2023). Is the hyoid a constraint on innovation? A study in convergence driving feeding in fish-shaped marine tetrapods. *Paleobiology*, *49*(4), 684–699. https://doi.org/10.1017/pab.2023.12

Druckenmiller, P. S. (2002). Osteology of a new plesiosaur from the lower Cretaceous (Albian) Thermopolis Shale of Montana. *Journal of Vertebrate Paleontology*, *22*(1), 29–42. https://doi.org/10.1671/0272-4634(2002)022[0029:OOANPF]2.0.CO;2

Gasparini, Z., Bardet, N., & Iturralde-Vinent, M. (2002). A new cryptoclidid plesiosaur from the Oxfordian (Late Jurassic) of Cuba. *Geobios*, *35*(2), 201–211. doi:10.1016/S0016-6995(02)00019-0

Gasparini, Z., Bardet, N., Martin, J. E., & Fernández, M. S. (2003). The elasmosaurid plesiosaur *Aristonectes cabrera* from the latest Cretaceous of South America and Antarctica. *Journal of Vertebrate Paleontology*, *23*(2), 104–115. doi:10.1671/0272-4634(2003)23[104:TEPACF]2.0.CO;2

Goloboff, P., & Morales, M. (2023). TNT version 1.6, with a graphical interface for MacOS and Linux, including new routines in parallel. *Cladistics*, *39*(2), 144–153. https://doi.org/10.1111/cla.12524

Hesselbo, S. P., Ogg, J. G., & Ruhl, M. (2020). The Jurassic Period. In F. M. Gradstein, J. G. Ogg, M. D. Schmitz & G. M. Ogg (Eds.), *Geological Time Scale 2020, volume 2* (pp. 955-1021). Elsevier Science Publishing. https://doi.org/10.1016/B978-0-12-824360-2.00026-7

Kear, B. P. (2005). A new elasmosaurid plesiosaur from the Lower Cretaceous of Queensland, Australia. *Journal of Vertebrate Paleontology*, *25*(4), 792–805. https://doi.org/10.1671/0272-4634(2005)025[0792:ANEPFT]2.0.CO;2

Kear, B. P. (2006). Marine reptiles from the Lower Cretaceous of South Australia: elements of a high-latitude cold-water assemblage. *Palaeontology*, *49*(4), 837–856.

Ketchum, H. F., & Benson, R. B. J. (2010). Global interrelationships of Plesiosauria (Reptilia, Sauropterygia) and the pivotal role of taxon-sampling in determining the outcome of phylogenetic analyses. *Biological Reviews*, *85*(2), 361–392. doi:10.1111/j.1469-185X.2009.00107.x

Ketchum, H. F., & Benson, R. B. J. (2022). A new pliosaurid from the Oxford Clay Formation of Oxfordshire, UK. *Acta Palaeontologica Polonica*, *67*(2), 297–315. https://doi.org/10.4202/app.00887.2021

Knutsen, E. M., Druckenmiller, P. S., & Hurum, J. H. (2012a). Redescription and taxonomic clarification of '*Tricleidus' svalbardensis* based on new material from the Agardhfjellet Formation (Middle Volgian). *Norwegian Journal of Geology*, *92*, 175–186.

Knutsen, E. M., Druckenmiller, P. S., & Hurum, J. H. (2012b). Two new species of long-necked plesiosaurians (Reptilia, Sauropterygia) from the Upper Jurassic (Middle Volgian) Agardhfjellet Formation of central Spitsbergen. *Norwegian Journal of Geology*, *92*, 187–212.

Knutsen, E. M., Druckenmiller, P. S., & Hurum, J. H. (2012c). A new plesiosaurid (Reptilia-Sauropterygia) from the Agardhfjellet Formation (Middle Volgian) of central Spitsbergen, Norway. *Norwegian Journal of Geology*, *92*, 213–234.

Maddison, W. P., & Maddison, D. R. (2023). Mesquite: a modular system for evolutionary analysis. Version 3.81.

Marx, M. P., Mateus, O., Polcyn, M. J., Schulp, A. S., Gonçalves, A. O., & Jacobs, L. L. (2021). The cranial anatomy and relationships of *Cardiocorax mukulu* (Plesiosauria: Elasmosauridae) from Bentiaba, Angola. *PLoS ONE*, *16*(8), e0255773. https://doi.org/10.1371/journal.pone.0255773

Massare, J. A. (1987). Tooth morphology and prey preference of Mesozoic marine reptiles. *Journal of Vertebrate Paleontology*, *7*(2), 121–137. doi:10.1080/02724634.1987.10011647

Morgans-Bell, H. S., Coe, A. L., Hesselbo, S. P., Jenkyns, H. C., Weedon, G. P., Marshall, J. E. A., Tyson, R. V., & Williams, C. J. (2001). Integrated stratigraphy of the Kimmeridge Clay Formation (Upper Jurassic) based on exposures and boreholes in south Dorset, UK. *Geological Magazine*, *138*(5), 511–539. https://doi.org/10.1017/S0016756801005738

Mulder, E. W. A., Bardet, N., Godefroit, P., & Jagt, J. W. M. (2000). Elasmosaur remains from the Maastrichtian type area, and a review of latest Cretaceous elasmosaurs (Reptilia, Plesiosauroidea). *Bulletinde l'Institut Royal des Sciences Naturalles de Belgique, Sciences dela Terre*, *70*, 161–178.

O'Keefe, F. R. (2001). A cladistic analysis and taxonomic revision of the Plesiosauria (Reptilia: Sauropterygia). *Acta Zoologica Fennica*, *213*, 1–63.

O'Gorman, J. P., Gasparini, Z., & Spalletti, L. A. (2018). A new *Pliosaurus* species (Sauropterygia, Plesiosauria) from the Upper Jurassic of Patagonia: new insights on the Tithonian morphological disparity of mandibular symphyseal morphology. *Journal of Paleontology*, *92*(2), 240–253. https://doi.org/10.1017/jpa.2017.82

O'Keefe, F. (2002). The evolution of plesiosaur and pliosaur morphotypes in the Plesiosauria (Reptilia: Sauropterygia). *Paleobiology*, *28*(1), 101–112. https://doi.org/10.1666/0094-8373(2002)028<0101:TEOPAP>2.0.CO;2

O'Keefe, F. R., Otero, R. A., Soto-Acuña, S., O'Gorman, J. P., Godfrey, S. J., & Chatterjee, S. (2017). Cranial anatomy of *Mortuneria seymourensis* from Antarctica, and the evolution of filter feeding in plesiosaurs of the Austral Late Cretaceous. *Journal of Vertebrate Paleontology*, *37*(4), e1347570. https://doi.org/10.1080/02724634.2017.1347570

O'Keefe, F. R., & Street, H. P. (2009). Osteology of the cryptocleidoid plesiosaur *Tatenectes laramiensis*, with comments on the taxonomic status of the Cimoliasauridae. *Journal of Vertebrate Paleontology*, *29*(1), 48–57. https://doi.org/10.1671/039.029.0118

O'Keefe, F. R., & Wahl, W. J. (2003). Current taxonomic status of the plesiosaur *Pantosaurus striatus* from the Upper Jurassic Sundance Formation, Wyoming. *Paludicola*, *4*(2), 37–46.

Otero, R. A., Alarcón-Muñoz, J., Soto-Acuña, S., Rojas, J., Rojas, O., & Ortíz, H. (2020). Cryptoclidid plesiosaurs (Sauropterygia, Plesiosauria) from the Upper Jurassic of the Atacama Desert. *Journal of Vertebrate Paleontology*, *40*(1), e1764573. https://doi.org/10.1080/02724634.2020.1764573

Owen, R. (1860). On the orders of fossil and recent Reptilia, and their distribution through time. *Report of the British Association for the Advancement of Science*, *29*, 153–166.

Owen, R. (1869). Monograph on the British Fossil Reptilia from the Kimmeridge Clay III. *Monographs of the Palaeontographical Society*, *22*(98), 1–12. doi:10.1080/02693445.1869.12113233

Páramo-Fonseca, M. E., Benavides-Cabra, C. D., & Gutiérrez, I. E. (2018). A new large Pliosaurid from the Barremian (Lower Cretaceous) of Sáchica, Boyacá, Colombia. *Earth Sciences Research Journal*, *22*(4), 223–238. https://doi.org/10.15446/esrj.v22n4.69916

Páramo-Fonseca, M. E., Benavides-Cabra, C. D., & Gutiérrez, I. E. (2019). A new specimen of *Stenorhynchosaurus munozi* Páramo-Fonseca et al., 2016 (Plesiosauria, Pliosauridae), from the Barremian of Colombia: new morphological features and ontogenetic implications. *Journal of Vertebrate Paleontology*, *39*(4), e1663426. https://doi.org/10.1080/02724634.2019.1663426

Pearson, S. J., Marshall, J. E. A. & Kemp, A. E. S. (2004). The White Stone Band of the Kimmeridge Clay Formation, an integrated high-resolution approach to understanding environmental change. *Journal of the Geological Society 161*(4), 675–683. https://doi.org/10.1144/0016-764903-089

Roberts, A. J., Druckenmiller, P. S., Cordonnier, B., Delsett, L. L., & Hurum, J. H. (2020). A new plesiosaurian from the Jurassic–Cretaceous transitional interval of the Slottsmøya Member (Volgian), with insights into the cranial anatomy of cryptoclidids using computed tomography. *PeerJ*, *8*, e8652. https://doi.org/10.7717/peerj.8652

Roberts, A. J., Druckenmiller, P. S., Delsett, L. L., & Hurum, J. H. (2017). Osteology and relationships of *Colymbosaurus* Seeley, 1874, based on new material of *C. svalbardensis* from the Slottsmøya Member, Agardhfjellet Formation of central Spitsbergen. *Journal of Vertebrate Paleontology*, *37*(1), https://doi.org/10.1080/02724634.2017.1278381

Sachs, S. (2005). *Tuarangisaurus australis* sp. nov. (Plesiosauria: Elasmosauridae) from the Lower Cretaceous of northeastern Queensland, with additional notes on the phylogeny of the Elasmosauridae. *Memoirs of the Queensland Museum*, *50*(2), 425–440.

Schumacher, B. A., & Martin, J. E. (2015). *Polycotylus latipinnis* Cope (Plesiosauria, Polycotylidae), an early complete skeleton from the Niobrara Formation (Early Campanian) of southwestern South Dakota. *Journal of Vertebrate Paleontology*. e1031341

Serratos, D. J., Druckenmiller, P. S., & Benson, R. B. J. (2017). A new elasmosaurid (Sauropterygia, Plesiosauria) from the Bearpaw Shale (Late Cretaceous, Maastrichtian) of Montana demonstrates multiple evolutionary reductions of neck length within Elasmosauridae. *Journal of Vertebrate Paleontology*, *27*(2), e1278608. https://doi.org/10.1080/02724634.2017.1278608

Smith, A., & Vincent, P. (2010). A new genus of pliosaur (Reptilia: Sauropterygia) from the Lower Jurassic of Holzmaden, Germany. *Palaeontology*, *53*(5), 945–1200. https://doi.org/10.1111/j.1475-4983.2010.00975.x

Stokke, M. K. (2022). *A large long-necked plesiosaur from the Late Jurassic Agardhfjellet Formation of central Spitsbergen, Norway.* [Unpublished master thesis]. University of Oslo.

Storrs, G. W., & Taylor, M. A. (1996). Cranial anatomy of a new plesiosaur genus from the lowermost Lias (Rhaetian/Hettangian) of Street, Somerset England. *Journal of Vertebrate Paleontology*, *16*(3), 403–402. https://doi.org/10.1080/02724634.1996.10011330

Taylor, M. A. (1992). Functional anatomy of the head of the large aquatic predator *Rhomaleosaurus zetlandicus* (Plesiosauria, Reptilia) from the Toarcian (Lower Jurassic) of Yorkshire, England. *Philosophical Transactions of the Royal Society of London. Series B: Biological Sciences*, *335*(1274), 247–280. https://doi.org/10.1098/rstb.1992.0022

Vincent, P. (2011). A re-examination of *Hauffiosaurus zanoni*, a pliosauroid from the Toarcian (Early Jurassic) of Germany. *Journal of Vertebrate Paleontology*, *31*(2), 340–351. https://doi.org/10.1080/02724634.2011.550352

Vincent, P., Bardet, N., Pereda-Suberbiola, X., Bouya, B., Amaghzaz, M., & Meslouh, S. (2011). *Zarafasaura oceanis*, a new elasmosaurid (Reptilia: Sauropterygia) from the Maastrichtian phosphates of Morocco and the palaeobiogeography of latest Cretaceous plesiosaurs. *Gondwana Research*, *19*(4), 1062–1073. https://doi.org/10.1016/j.gr.2010.10.005

Weedon, G., Coe, A., & Gallois, R. (2004). Cyclostratigraphy, orbital tuning and inferred productivity for the type Kimmeridge Clay (Late Jurassic), Southern England. *Journal of the Geological Society*, *161*(4), 655–666. https://doi.org/10.1144/0016-764903-073

Welles, S. P. (1943). Elasmosaurid plesiosaurs with description of new material from California and Colorado. *Memoirs of University of California*, *13*, 125–254.

Williston, S. W. (1925). Osteology of the Reptiles. Harvard University Press, Cambridge, Massachusetts, 300 pp.

Wintrich, T., Hayashi, S., Houssaye, A., Nakajima, Y., & Sander, P. M. (2017). A Triassic plesiosaurian skeleton and bone histology inform on evolution of a unique body plan. *Science Advances*, *3*(12), e1701144. https://doi.org/10.1126/sciadv.1701144

Handling Editor: Daniel Madzia.
Phylogenetics Editor: Daniel Casali.